

Modelling of the penetration process of externally applied magnetic perturbation of the DED on TEXTOR

Y. Kikuchi^{1,a}, K.H. Finken¹, D. Reiser¹, G. Sewell², M. Jakubowski¹, M. Lehnen¹

¹ *Institut fuer Plasmaphysik, Forschungszentrum Juelich GmbH, D-52425, Germany*

² *Mathematics Dept. Texas A&M University, College Station, Texas, USA*

^a *JSPS Postdoctoral Fellowships for Research Abroad*

1 Introduction

The error-field penetration process into a rotating tokamak plasma has been studied on the TEXTOR tokamak. In the TEXTOR tokamak a set of external perturbation coils, the so called Dynamic Ergodic Divertor (DED), are installed [1]. The unique feature of the DED is the capability to apply rotating helical magnetic perturbation fields with a frequency of up to 10 kHz. The penetration process of the perturbation field modifies poloidal flux and creates the mode, so that the DED leads to the excitation of a tearing mode in spite of $\Delta'_0 < 0$ (Δ'_0 : tearing stability index) when the amplitude of the DED exceeds a certain threshold [2]. In this paper, we investigate the dynamics of the penetration process of the DED into rotating tokamak plasmas in terms of a quasi-linear MHD simulation in order to understand the experimental results on TEXTOR.

2 Model equations

We employ the following linearized reduced set of single fluid resistive and viscous MHD equations in a low β cylindrical tokamak plasma. The standard right-hand cylindrical polar co-ordinates (r, θ, z) are adopted. The plasma is assumed to be periodic in the z direction with periodicity length $2\pi R_0$, where R_0 is the simulated major radius. The equilibrium magnetic field and velocity are written as

$$\mathbf{B}_0 = (0, B_{\theta 0}(r), B_{z0}), \quad \mathbf{v}_0 = (0, v_{\theta 0}(r), v_{z0}(r)). \quad (1)$$

By introducing a perturbed magnetic flux $\tilde{\psi}$ and a perturbed stream function $\tilde{\phi}$, the perturbed magnetic field and velocity are described as

$$\tilde{\mathbf{B}} = \nabla \tilde{\psi} \times \mathbf{e}_z = \left(\frac{im}{r} \tilde{\psi}, -\frac{\partial \tilde{\psi}}{\partial r}, 0 \right), \quad \tilde{\mathbf{v}} = \nabla \tilde{\phi} \times \mathbf{e}_z = \left(\frac{im}{r} \tilde{\phi}, -\frac{\partial \tilde{\phi}}{\partial r}, 0 \right), \quad (2)$$

where an $\exp[i(m\theta - nz/R_0)]$ dependence of the perturbed quantities is assumed. The differential equations for the perturbed quantities can be written as following;

$$\begin{aligned} \frac{\partial \tilde{U}}{\partial t} = & \frac{im}{\rho \mu_0 r} \left\{ B_{\theta 0} (1 - nq/m) \Delta_{\perp} \tilde{\psi} - \mu_0 \frac{\partial j_{z0}}{\partial r} \tilde{\psi} \right\} + \frac{\mu_{\perp}}{\rho} \Delta_{\perp} \tilde{U} \\ & - \left(\frac{im}{r} v_{\theta 0} - \frac{in}{R_0} v_{z0} \right) \tilde{U} + \frac{in}{R_0} \frac{\partial v_{z0}}{\partial r} \frac{\partial \tilde{\phi}}{\partial r} + \frac{im}{r} \left(\frac{\partial^2 v_{\theta 0}}{\partial r^2} + \frac{1}{r} \frac{\partial v_{\theta 0}}{\partial r} - \frac{1}{r^2} v_{\theta 0} \right) \tilde{\phi}, \end{aligned} \quad (3)$$

$$\frac{\partial \tilde{\psi}}{\partial t} = \frac{\eta}{\mu_0} \Delta_{\perp} \tilde{\psi} + \frac{im}{r} B_{\theta 0} (1 - nq/m) \tilde{\phi} - \left(\frac{im}{r} v_{\theta 0} - \frac{in}{R_0} v_{z0} \right) \tilde{\psi}, \quad (4)$$

$$\tilde{U} = \Delta_{\perp} \tilde{\phi}, \quad \Delta_{\perp} = \frac{1}{r} \frac{\partial}{\partial r} \left(r \frac{\partial}{\partial r} \right) - \frac{m^2}{r^2}, \quad (5)$$

where ρ , μ_0 , μ_{\perp} , η , \tilde{U} are the plasma mass density, the permeability of free space, the plasma perpendicular viscosity, the plasma resistivity and the perturbed vorticity,

respectively. Non-linearities are included in terms of the following quasi-linear approach.

$$\begin{aligned} \frac{\partial B_{\theta 0}}{\partial t} &= \frac{1}{\mu_0} \frac{\partial}{\partial r} \left(\frac{\eta}{r} \frac{\partial}{\partial r} (r(B_{\theta 0} - B_{\theta 0}|_{t=0})) \right) \\ &+ \frac{1}{2} \Im_m \left[\frac{m}{r^2} \left(\tilde{\psi}^* \frac{\partial \tilde{\phi}}{\partial r} + \tilde{\phi} \frac{\partial \tilde{\psi}^*}{\partial r} \right) - \frac{m}{r} \left(\tilde{\psi}^* \frac{\partial^2 \tilde{\phi}}{\partial r^2} + \tilde{\phi} \frac{\partial^2 \tilde{\psi}^*}{\partial r^2} + 2 \frac{\partial \tilde{\phi}}{\partial r} \frac{\partial \tilde{\psi}^*}{\partial r} \right) \right], \end{aligned} \quad (6)$$

$$\begin{aligned} \rho \frac{\partial v_{\theta 0}}{\partial t} &= \frac{1}{r^2} \frac{\partial}{\partial r} \left(\mu_{\perp} r^3 \frac{\partial}{\partial r} \left(\frac{1}{r} (v_{\theta 0} - v_{\theta 0}|_{t=0}) \right) \right) - \rho \mu_{\parallel} (v_{\theta 0} - v_{\theta 0}|_{t=0}) \\ &- \frac{m}{2\mu_0 r} \Im_m (\tilde{\psi}^* \Delta_{\perp} \tilde{\psi}) - \frac{\rho m}{2r} \Im_m \left(\tilde{\phi} \frac{\partial^2 \tilde{\phi}^*}{\partial r^2} - \frac{1}{r} \tilde{\phi}^* \frac{\partial \tilde{\phi}}{\partial r} \right), \end{aligned} \quad (7)$$

$$\begin{aligned} \rho \frac{\partial v_{z 0}}{\partial t} &= \frac{1}{r} \frac{\partial}{\partial r} \left(\mu_{\perp} r \frac{\partial}{\partial r} (v_{z 0} - v_{z 0}|_{t=0}) \right) \\ &+ \frac{n}{2\mu_0 R_0} \Im_m (\tilde{\psi}^* \Delta_{\perp} \tilde{\psi}) + \frac{\rho n}{2R_0} \Im_m \left(\tilde{\phi} \frac{\partial^2 \tilde{\phi}^*}{\partial r^2} - \frac{1}{r} \tilde{\phi}^* \frac{\partial \tilde{\phi}}{\partial r} \right), \end{aligned} \quad (8)$$

where μ_{\parallel} , superscript $*$ and \Im_m are the neoclassical parallel viscosity in the poloidal direction ($\sim 7 \times 10^5 \text{ s}^{-1}$), the conjugate complex and the imaginary part of the complex value, respectively.

For the numerical treatment, the present time-dependent and one-dimensional problem of the above differential equations were solved by PDE2D code (finite element solver) [3] with the following boundary conditions. The computational domain includes vacuum regions between the plasma and the DED coil, and outside the DED coil. The perturbations are assumed to be continuous at the transition of the different areas. At the axis ($r = 0$) and at infinity ($r = 10 \text{ m}$) the perturbations are set to zero. The $\tilde{\phi}$ is set to be zero outside the plasma region ($r > a$, a : plasma radius). The DED coil current is assumed to be a form of $\exp i(m\theta - nz/R_0 - \omega_{DED}t)$, where ω_{DED} is the angular frequency of the DED. Here, the Doppler-shifted angular frequency of the DED with respect to the rotating plasma is written as $\omega' = \omega_{DED} - \{(m/r)v_{\theta 0} - (n/R_0)v_{z 0}\}$. The initial profile of the equilibrium current density is taken as $j_{z 0} = (\nu + 1)I_p(1 - (r/a)^2)^{\nu} / \pi a^2$. Here, I_p and ν are the plasma current and the peaking factor of $j_{z 0}$, respectively.

3 Numerical results

3.1 Linear calculations

The strong $m/n = 2/1$ sideband component which is created by the DED configuration of the $m/n = 3/1$ is considered in this paper. The plasma current, the toroidal magnetic field, the electron temperature and density at $q = 2$ are set to 300 kA, 2.25 T, 500 eV, and $2 \times 10^{19} \text{ m}^{-3}$, respectively. The skin depth $\delta (= \sqrt{\eta / (\mu_0 \omega_{DED})})$ of the DED-field in the case of 1 kHz and the Lundquist number $S (= \tau_R / \tau_A, \tau_R$: the current diffusion time, τ_A : the Alfvén wave transit time) are 3.2 mm and 6×10^7 , respectively. Figure 1 shows the radial profiles of the $\tilde{\psi}$, where the DED frequency, the plasma rotation and the plasma viscosity are set to zero. The amount of the error-field amplification with respect to the vacuum field depends on the initial current density profile (i.e., Δ'_0). When increasing the DED frequency, the amplification of the $\tilde{\psi}$ at $q = 2$ is suppressed by an eddy current flow near the resonance layer as shown in Fig. 2. When the Doppler-shifted frequency of the DED is very high, the contributions of the

Alfvén resonances on the penetration process of the DED into the tokamak plasma are not hindered in comparison with the dissipation due to the plasma resistivity as shown in Fig. 3. In this case, the magnetic reconnection at $q = 2$ is strongly suppressed. However, the two peaks of the observed perturbed current density \tilde{j}_z are overlapped due to a finite plasma viscosity. Here, the perpendicular viscosity μ_{\perp} is set to a large value compared with the neoclassical one $\mu_{\perp 0}(= 7.8 \times 10^{-10} \text{ kg} \cdot \text{m}^{-1} \cdot \text{s}^{-1})$.

3.2 Quasi-linear calculations

In order to clarify the nonlinear behaviour of the error-field penetration process, the quasi-linear calculations have been performed, in which the changes of the equilibrium poloidal field (eq.(6)) and the plasma rotation velocity profiles (eqs(7),(8)) due to the perturbation field are taken into account. Figure 4 shows the typical result of the time development of the plasma toroidal rotation and the $\tilde{\psi}$ at $q = 2$, where the DED coil current is ramped up linearly in time, and the $v_{\theta 0}$ is neglected. The corresponding radial profile of the $v_{z 0}$ is shown in Fig. 5. The rotation braking gives rise to the bifurcation of the penetration process from the suppressed to the excited state, because the amount of the magnetic reconnection depends strongly on the Doppler-shifted frequency of the magnetic perturbation with respect to the rotating plasma. On the other hand, the effect of the plasma poloidal rotation on the penetration process of the magnetic perturbation is same as that of the toroidal rotation except the strong damping of the poloidal rotation due to the μ_{\parallel} . Figure 6 shows the dependence of the threshold for the bifurcation of the penetration process on the $v_{z 0}$, where the $v_{\theta 0}$ is set to 0 or 1.9 km/s at $q = 2$. It is shown that the contribution of the poloidal rotation on the threshold of the bifurcation cannot be neglected, although the $v_{\theta 0}$ is much smaller than the $v_{z 0}$.

4 Summary and discussions

In order to understand the underlying physics, a single fluid MHD simulation code has been developed, taking into account the plasma resistivity and viscosity. A quasi-linear calculation shows that a sudden growth of the magnetic reconnection arises with changes of the plasma rotation. In the real experiment on TEXTOR it is found that the threshold for the mode onset is asymmetrical during co- and ctr-injected (with respect to the direction of the plasma current) tangential neutral beam, although the absolute value of the toroidal rotation velocity is the same, only the direction is changed [2]. Further investigations about the above behaviour are necessary, but the contribution of the poloidal rotation on the threshold for the error-field penetration as shown in this study could be one of the possible reasons.

References: [1] K. H. Finken et al., Phys. Rev. Lett. **94** (2005) 015003., [2] H. R. Koslowski et al., 31st EPS Conf. Plasma Physics (London) P1-124., and this conference (P4.061)., [3] G. Sewell, <http://www.pde2d.com>.

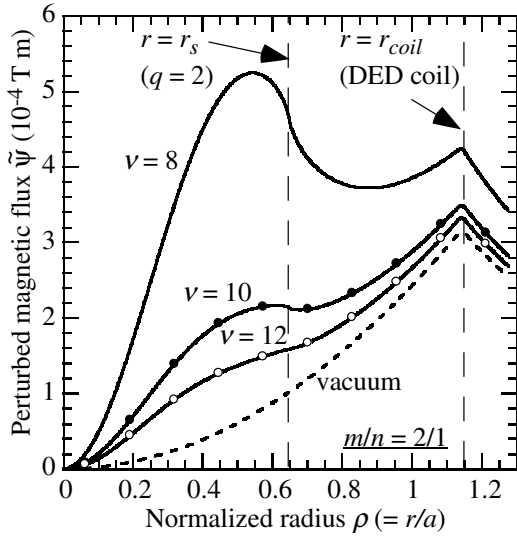


Fig. 1 Radial profiles of the perturbed magnetic flux $\tilde{\psi}$ in the cases of $\nu = 8$ ($\Delta_0' = -3.0$), 10 ($\Delta_0' = -5.2$) and 12 ($\Delta_0' = -8.4$). The f_{DED} is set to zero (DC-DED).

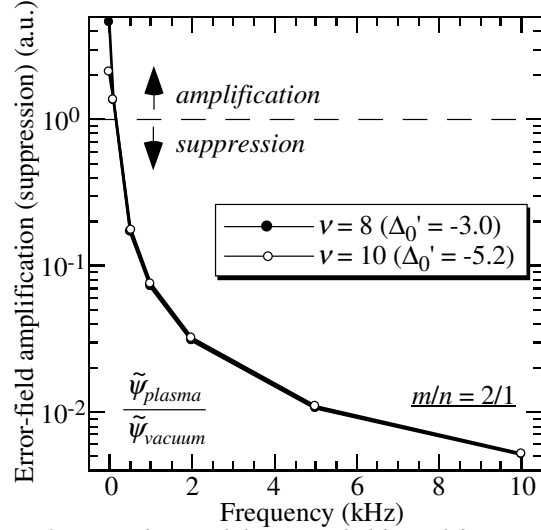


Fig. 2 Dependence of the error-field amplification (suppression) on the DED frequency, where μ_{\perp} , $\nu_{\theta 0}$ and $\nu_{z0} = 0$.

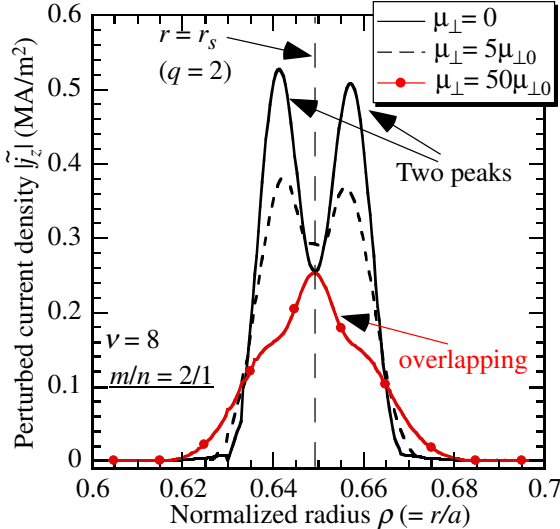


Fig. 3 Effects of the viscosity on the Alfvén resonances, where $f_{DED} = 10$ kHz, $\nu_{\theta 0} = -5$ km/s and $\nu_{z0} = 40$ km/s.

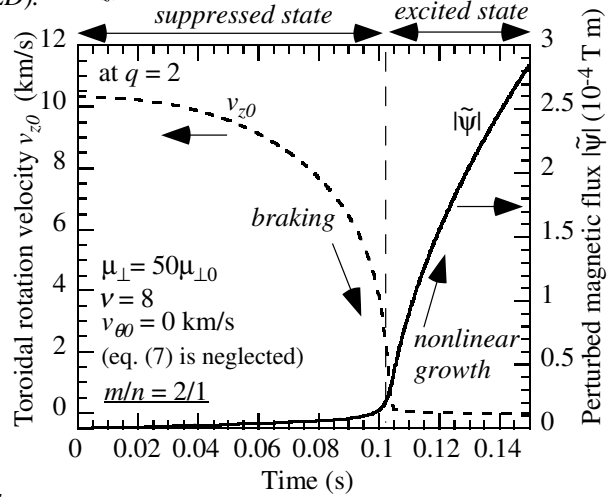


Fig. 4 Time developments of the $\tilde{\psi}$ and the ν_{z0} at $q = 2$. The DED current is linearly ramped up in time. The f_{DED} is set to zero (DC-DED).

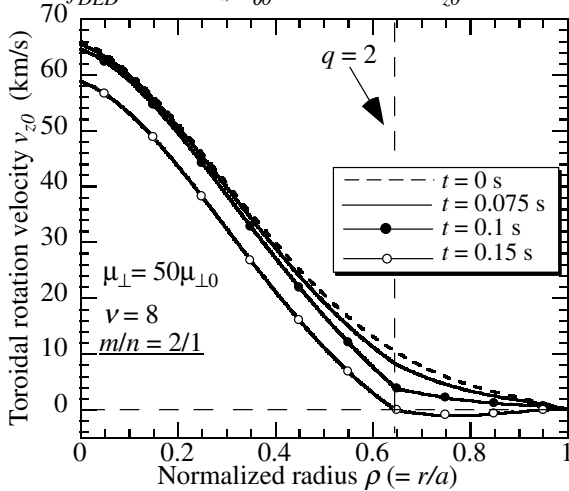


Fig. 5 Time developments of the radial profiles of the ν_{z0} . The condition is same as shown in fig. 4.

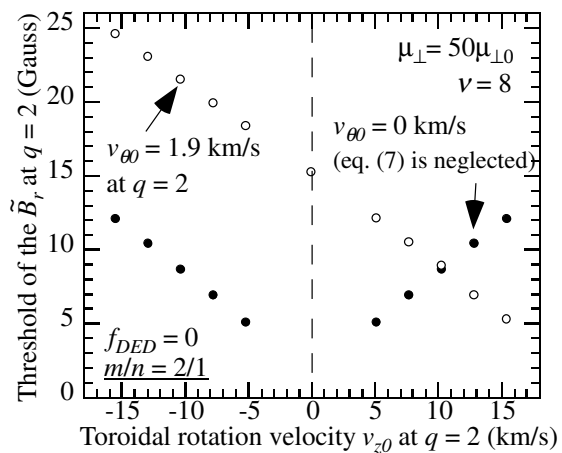


Fig. 6 Dependences of the threshold of the \tilde{B}_r for the mode penetration on the ν_{z0} (\bullet : eq. (7) is neglected, \circ : $\nu_{\theta 0} = 1.9$ km/s at $q = 2$).